Acta Crystallographica Section B
Structural Science
ISSN 0108-7681
Editor: **Carolyn P. Brock**

Charge-density analysis of the ground state of a photochromic 1,10-phenanthroline zinc(II) bis(thiolate) complex

Stephan Scheins, Shao-Liang Zheng, Jason B. Benedict and Philip Coppens

Acta Cryst. (2010). B**66**, 366–372

Acta Crystallographica Section B: Structural Science publishes papers in structural chemistry and solid-state physics in which structure is the primary focus of the work reported. The central themes are the acquisition of structural knowledge from novel experimental observations or from existing data, the correlation of structural knowledge with physicochemical and other properties, and the application of this knowledge to solve problems in the structural domain. The journal covers metals and alloys, inorganics and minerals, metal-organics and purely organic compounds.

Acta Crystallographica Section B
Structural Science
ISSN 0108-7681

Charge-density analysis of the ground state of a photochromic 1,10-phenanthroline zinc(II) bis(thiolate) complex

Stephan Scheins, Shao-Liang Zheng, Jason B. Benedict and Philip Coppens*

Chemistry Department, University at Buffalo, SUNY, Buffalo, NY 14260-3000, USA

Correspondence e-mail: coppens@buffalo.edu

Received 9 October 2009
Accepted 15 March 2010

The charge density of the title compound was determined at 90 K, using a spherical crystal of 150 μm diameter. The proper treatment of the Zn atom in the pseudo-tetrahedral environment is considered in detail. A satisfactory refinement is only obtained when anharmonic Gram–Charlier parameters are included as variables in the refinement. A successful combined anharmonic/multipole refinement indicates a small polarization of the 4*s* shell in the anisotropic environment. One of the two toluenethiols is approximately π-stacked with the phenanthroline ligand. A bond path is found connecting the two ligands. In addition the Zn—S bond to this ligand is slightly extended compared with the same bond to the second toluenethiol. A separate photocrystallographic and theoretical study indicates the long wavelength emission of the title compound to be due to a ligand-to-ligand charge transfer (LLCT) from a toluenethiol to the phenanthroline ligand. The charge-density results do not provide a basis for deciding which of the thiole ligands is the source of the transferred electron density. This result is in agreement with the theoretical calculations, which show comparable oscillator strengths for charge transfer from either of the ligands.

1. Introduction

In a series of publications Crosby and coworkers reported the intriguing spectroscopic behavior of a series of substituted 1,10-phenanthrolines zinc(II) bis(thiolates) (Fig. 1; Highland *et al.*, 1986; Cremers *et al.*, 1980; Jordan *et al.*, 2002; Crosby *et al.*, 1985). In rigid glasses and crystals at low temperatures the complexes exhibit a dual luminescence consisting of a diffuse long wavelength band (~ 1700 cm^{-1}) with a μs lifetime and a shorter wavelength, structured band with a lifetime of almost 1 s at 77 K in rigid glasses. The bands were assigned to a $\pi \rightarrow \pi^*$ transition on the phenanthroline and an LLCT from the toluenethiol ligands to the heterocyclic phenanthroline, The spectroscopy and electrochemistry of the dithienyl-substituted

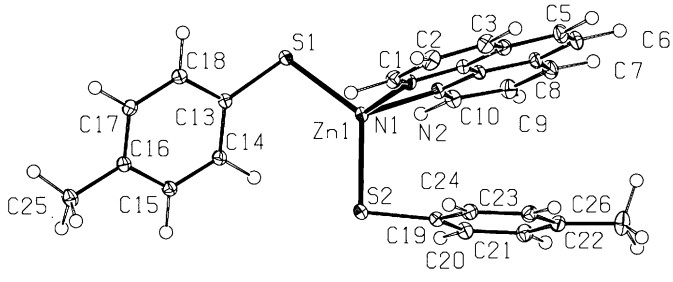

Figure 1
Diagram of (1) and labeling of atoms.

Table 1
Experimental details.

Crystal data	
Chemical formula	$C_{26}H_{22}N_2S_2Zn$
M_r	491.99
Crystal system, space group	Monoclinic, $P2_1/c$
Temperature (K)	90
a, b, c (Å)	9.9280 (4), 19.9226 (8), 12.0100 (5)
β	107.924 (1)
V (Å^3)	2260.18 (16)
Z	4
Radiation type	Mo $K\alpha$
μ (mm^{-1})	1.29
Crystal size (mm)	0.15 (radius)
Data collection	
Diffractometer	Bruker SMART Apex II CCD Detector
Absorption correction	Empirical (using intensity measurements) spherical
T_{min}, T_{max}	0.754, 0.781
No of measured, independent and observed reflections	293 231, 26 207, 21 306
Completeness (%)	99.8
Redundancy	11.2
$(\sin\theta/\lambda)_{max}$ (Å^{-1})	1.114
R_{int}† (%)	3.95
Refinement	
$R[F^2 > 2\sigma(F^2)]$, $wR(F^2)$, S	0.014, 0.017, 0.92
$R1$ (*SHELX*)	0.0222
$R1$ (XD, refinement 3)	0.0140
No. of reflections	21 306
No. of parameters	837
No. of restraints	0
H-atom treatment	H-atom parameters constrained
$\Delta\rho_{max}$, $\Delta\rho_{min}$ (e Å^{-3})	0.30/−0.36

Computer programs used: *SORTAV* (Blessing, 1997), *SHELXS*97 (Sheldrick, 2008), *XD*2006 (Volkov *et al.* (2006). † Data averaged in *SORTAV*, R_{int} with *SADABS* and *SORTAV* equals 2.88%.

complexes have been described recently by Yam and coworkers (Ngan *et al.*, 2007).

In parallel to a photocrystallographic study to be reported separately, we performed a charge-density analysis of the ground state of bis(4-methylbenzenethiolato)(1,10-phenanthroline)zinc(II) (1) to evaluate the net charges on the ligands and examine the charge distribution of the Zn atom. The latter is found to be especially elusive, as described in detail below.

2. Experimental

Complex (1) was synthesized and crystals were grown following a procedure described in the literature (Ngan *et al.*, 2007). A crystal to be used for data collection was ground to a sphere of 150 µm diameter with a Nonius crystal grinder. X-ray data were collected with Mo $K\alpha$ radiation on a rotating anode generator at 90 K and a Bruker-Apex II area detector, with a crystal–detector distance of 4 cm. Nineteen different sets of data were collected, 17 of them covering a 180° ω range with a step size of 0.3°, including one low-order run collected with a decreased generator power setting to avoid loss of reflection intensities by saturation of the detector. In addition, two sets of φ scans were collected covering a 360° range. The *APEX*II software (Bruker, 1999*a*,*b*) was used for data collection and integration, while the data were merged with the program *SORTAV* (Blessing, 1997).

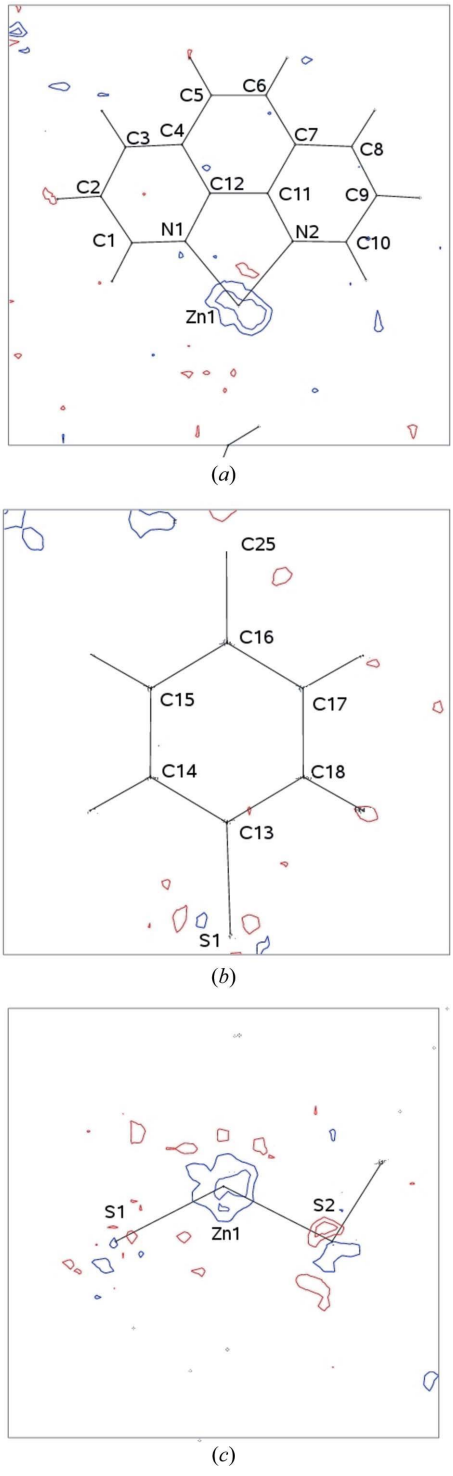

Figure 2
Residual maps in the plane of (*a*) the phenanthroline ring, (*b*) the *para*-toluenethiol ring and (*c*) the plane containing S1—Zn1—S2 after refinement 1. Contours at 0.1 e Å^{-3}, blue/red: positive/negative. Zero contours omitted.

Table 2
Significant (>3σ) anharmonic displacement parameters on the Zn atom, refinements 2 and 3.

Parameter	Refinement 2	Refinement 3	σ
*C*111	0.000027	0.000028	0.000006
*C*112	0.000014	0.000014	0.000002
*C*122	0.000005	0.000006	0.000001
*C*113	−0.000008	−0.000008	0.000002
*D*1111	0.000070	0.000070	0.000004
*D*3333	0.000015	0.000014	0.000002
*D*1113	0.000013	0.000013	0.000002
*D*1333	0.000015	0.000015	0.000001
*D*1133	0.000011	0.000011	0.000001

The crystallographic information is summarized in Table 1.[1]

The extent and accuracy of the data set allowed refinement of the aspherical density distribution according to the Hansen–Coppens formalism (Hansen & Coppens, 1978) as coded in the program *XD* (Volkov *et al.*, 2006). As a starting point of the refinement the independent atom model was used. To analyze an anomaly in the Zn charge distribution, three different refinements were performed. In all refinements the multipoles were introduced in a stepwise manner, with first only monopoles, then monopoles and dipoles *etc.* until a full hexadecapole expansion was reached. The κ parameter of the Zn atom was fixed at 1, as attempts to refine this parameter led to unrealistic values. H atoms were treated isotropically in all refinements.

2.1. Refinement 1

The two 4*s* electrons of the Zn atom were included in the core and not refined, while the *d* electrons populated the valence shell. For H atoms the multipole expansion was truncated at the dipolar level. In the final stage the κ expansion–contraction parameters were refined for non-H atoms, while the κ parameters for the H atoms were fixed at 1.2. The reflection-to-parameter ratio in the final refinement was 26.0. The refinement converged with a final agreement factor of $R1 = 0.0145$. The featureless residual density maps ($-0.36 \leq \Delta\rho \leq 0.32$ e Å^{-3}) including all reflections, shown in Fig. 2, indicate an adequate fit of the multipole model to the experimental data. The Hirshfeld rigid-bond test (Hirshfeld, 1976) shows the largest difference of mean-squares displacement amplitudes in the bond directions as 0.0006 Å^2, suggesting a proper deconvolution of thermal motion and bonding effects.

While the fit obtained in this refinement is satisfactory two anomalies resulted. First, the net charge on the Zn atom was negative with a charge of −0.59 e according to the multipole refinement (*d*-orbital population 10.594 e), and −0.55 e according to the Hirshfeld analysis of the results. Second, the deformation density from this refinement shows a pronounced deviation from spherical symmetry which is unexpected for a Zn atom (Fig. 3), although the ligand planes showed no unusual features. Both features are in contradiction with the distribution expected for a full-shell Zn atom which is supposed to have a spherical electron density, and the metallic character of Zn. They are also not supported by the theore-

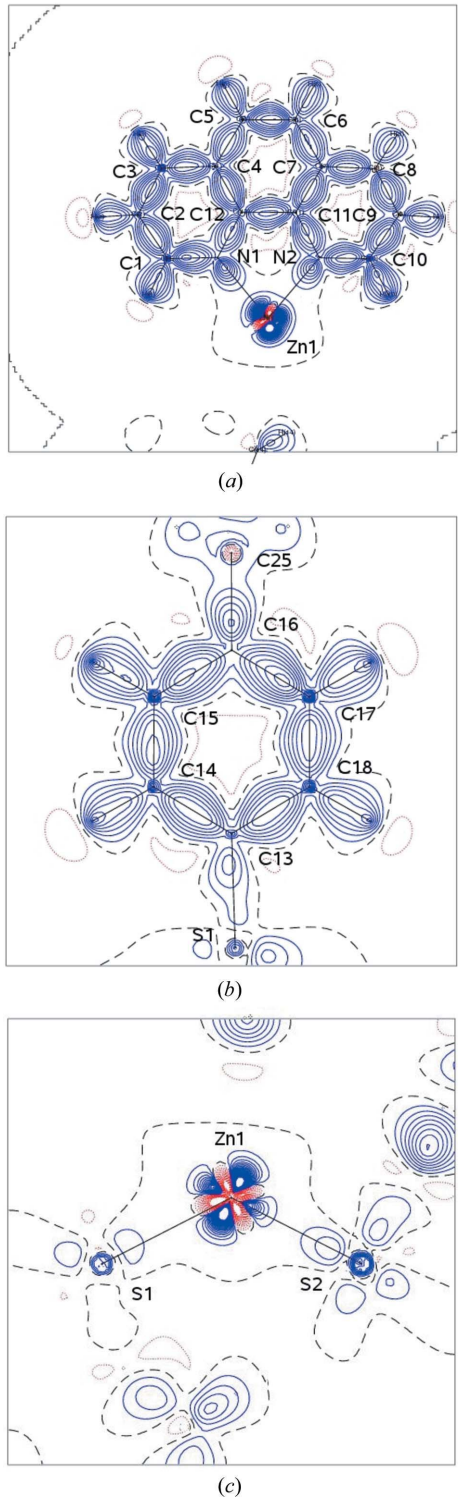

Figure 3
Experimental deformation density maps in the plane of the phenanthroline (I), the *para*-toluenethiol (II) ring system and the plane containing S1—Zn1—S2 (contours at 0.1 e Å^{-3}, blue/red: positive/negative, zero contours broken).

[1] Supplementary data for this paper are available from the IUCr electronic archives (Reference: PI5004). Services for accessing these data are described at the back of the journal.

Table 3
Correlation coefficients > 0.60 in refinement 3.

Variables	Correlation coefficients	Variables	Correlation coefficients
X–*C*111	76	*U*13–*D*1133	67
Y–*C*222	75	*U*23–*D*2223	69
Z–*C*333	74	*U*23–*D*2333	68
*U*11–*D*1111	89	*C*333–*C*133	61
*U*22–*D*2222	87	*C*113–*C*133	67
*U*33–*D*3333	88	*D*1111–*D*1113	64
*U*12–*D*1112	69	*D*3333–*D*1333	65
*U*12–*D*1222	70	*D*1113–*D*1133	76
*U*13–*D*1113	77	*D*1333–*D*1133	77
*U*13–*D*1333	77	*D*1123–*D*1233	65

tical results described below. A second refinement was therefore performed

2.2. Refinement 2

In the second refinement only the 4*s* multipole was included in the Zn valence shell. All higher poles centered on Zn were omitted. The refinement clearly showed residual features owing to the high-order data, as illustrated in Fig. 4, indicative of thermal motion. Anharmonicity was introduced for the Zn thermal vibrations by including Gram–Charlier parameters up to fourth order. This strategy is similar to refinements on Zn compounds described by Ghermani and co-workers (Spasojevic de Bire *et al.*, 2002; Novakovic *et al.*, 2007).

This refinement leads to a positive charge of +0.85 e on the spherical Zn atom with a final *R* factor of 0.0142, essentially identical to that of refinement 1. In particular, the *D*1111 parameter has a value equal to almost 20 times his respective standard deviations (Table 2). Relevant maps are shown in Figs. 4 and 5. The resulting net charges on the Zn atom are +0.85 (6) e from the multipole population and +0.37 e from the Hirshfeld analysis.

2.3. Combined anharmonic/multipole refinement 3

Both the Zn multipoles of the 4*s* valence density and the higher-order displacement parameters were included in a subsequent refinement. It converged at an *R* factor of 0.0140, essentially identical to those of refinements 2 and 3, although the number of variables in this refinement is larger. The net charge on the Zn of +0.88 e is essentially unchanged from that of refinement 2. Changes in the higher-order displacement parameters compared with refinement 2 are also minimal (Table 2). The multipole parameters suggest a slight polarization of the 4*s* density in the molecular environment, as illustrated in Fig. 5. Atomic, displacement and charge density parameters for the Zn and S atoms are listed in Table S1. Normal probability plots and information on the weighting scheme used are given in Figs. S1–S3 of the supplementary material.

As found in an earlier analysis of the Fe-atom asphericity in crystals of bis(pyridine)(*meso*-tetraphenylporphinato)iron(II) (Mallinson *et al.*, 1988), correlations exist between the refined variables. However, unlike in the 1988 study, the correlation coefficients in the current refinement are smaller, and do not involve the multipole population parameters (Table 3), likely reflecting the improved quality of the data compared with those collected more than 20 years ago.

3. Theoretical calculations

The *GAUSSIAN*09 program package was used for an *ab initio* calculation at the density functional (B3LYP) level of theory with a 6–311++G** basis set (Frisch *et al.*, 2009). A single point calculation at the experimental geometry was carried out for comparison with the experimental results. Aromatic and methyl-group C—H bonds were set at 1.083 and 1.059 Å, values essentially identical to those obtained in the multipole refinements. The wavefunctions obtained were evaluated with the program package *AIMPAC* (Cheeseman *et al.*, 1992). The

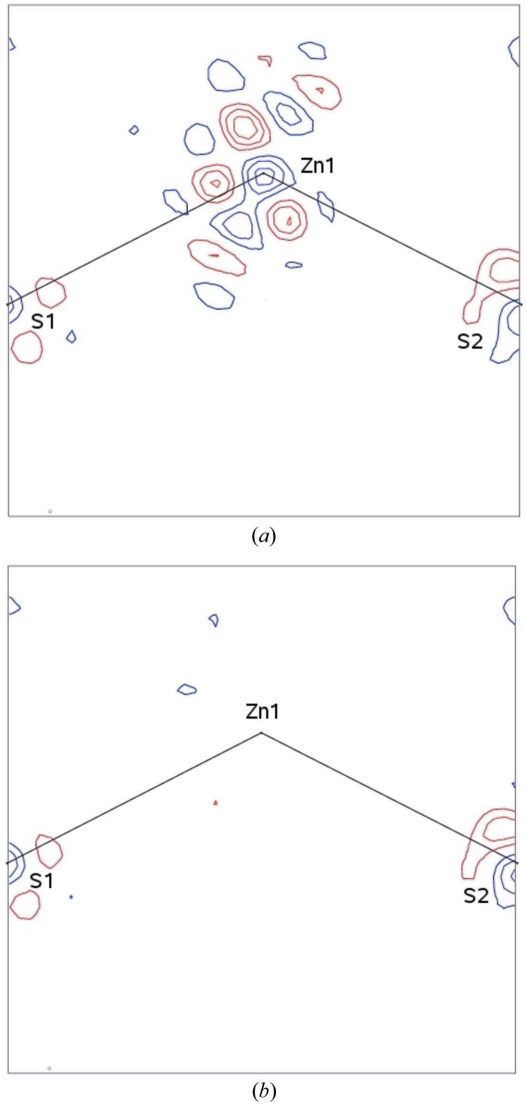

Figure 4
Residual maps: (*a*) after harmonic refinement 2, reflections with 0.8 < $\sin\theta/\lambda$ < 1.1 Å^{-1} only; (*b*) anharmonic refinement, all reflections. Contour as in Fig. 2.

Table 4
Comparison of experimental and theoretical charges (e) on the Zn atom.

	XD	Hirshfeld	Bader
Theory		+0.42	+0.97
Refinement 1	−0.59 (6)	−0.55	−0.21
Refinement 2	+0.85 (6)	+0.37	+1.13
Refinement 3	+0.88 (6)	+0.39	+1.10

theoretical deformation map in the S—Zn—S plane, calculated with the program *WFN2PLOTS* (Volkov, 2005), is compared with the experimental result (anharmonic refinement) in Fig. 5. Net atomic charges are summarized in Tables 4 and S2. The features of the two maps are very similar with the exception of the region close to the Zn nucleus where the charge deficiency is much more concentrated in the theoretical map. However, the net charges on the Zn listed in Table 4 are very close.

4. Topological analysis of the electron density

A full topological analysis (Bader, 1994) was performed with the *XDPROP* routine of the *XD* package (Volkov *et al.*, 2006). The theoretical density at the experimental geometry was analyzed with the program *AIMPAC* (Cheeseman *et al.*, 1992). Bond-critical points (BCPs) were found in all covalent bonds. The experimental and theoretical topological descriptors for all bonds are summarized in the supporting material section (Table S2). The agreement of the BCP properties between experiment and theory is very good for the aromatic CC and CN bonds in the complex (Table S2). For the two CS bonds and the heterocyclic CC bond involving the methyl group the agreement is very good for the electron density, whereas the theoretical values for the Laplacian are more negative than the experimental ones [−7.5 (1)/−3.4 (4) e Å^{-5}]. For the bonds involving the Zn atom, theory and experiment agree well on the electron density in the bond to S2, which is approximately π-stacked to the phenanthroline plane, while the experimental electron density at the BCP is somewhat smaller than the theoretical one for the Zn—S1 bond to the 'free' benzenethiol. Interestingly, the bond to the stacked ligand is stretched by 0.016 Å compared with the bond to the 'free' thiol' (Table 5). Further confirmation of the interaction between the two aromatic ring systems is provided by the existence of a BCP linking C24 of the thiolate ligand and N1 of the phenanthroline with ρ = 0.05 (1) e Å^{-3}, $\nabla^2\rho$ = 0.5 (1) e Å^{-5}, according to both theory and experiment, as illustrated in Fig. 6.

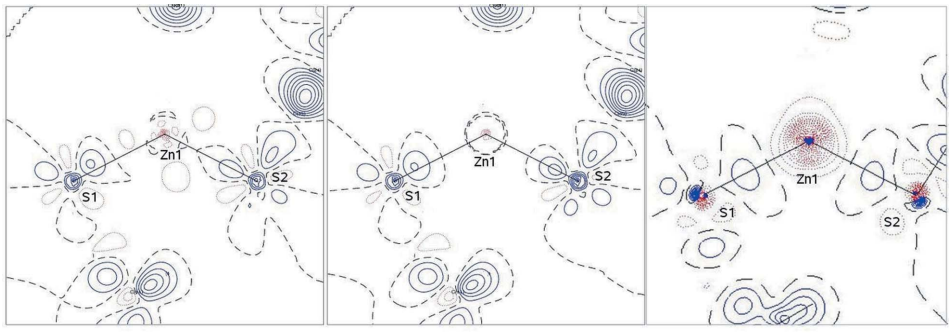

(*a*) (*b*) (*c*)

Figure 5
Deformation density maps in the S—Zn—S plane, (*a*) refinement 3, (*b*) refinement 2 and (*c*) theory; contours at 0.1 e Å^{-3}. Blue: excess density, red: deficient density. Zero contours broken.

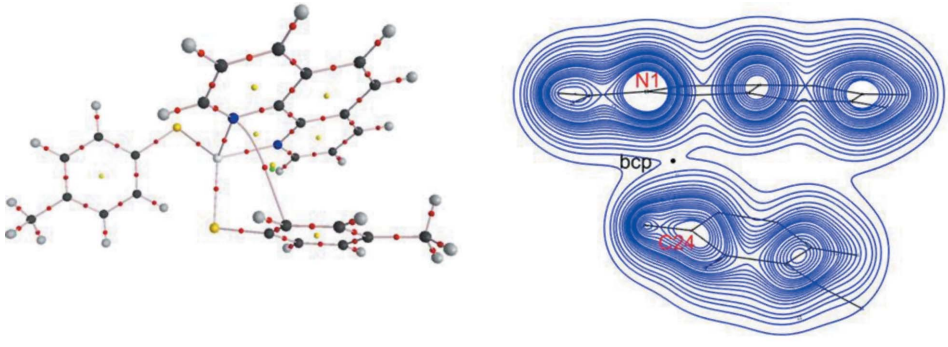

(*a*) (*b*)

Figure 6
(*a*) Molecular graph derived from theory, bond paths (orange), BCPs (red), ring-critical points (yellow); (*b*) contour plot of the experimental electron density viewed sideways approximately in the plane of the phenanthroline ligand, showing the experimental BCP in the bond path connecting the two ligands

A more detailed comparison of bonds is provided by the analysis of the local energy densities at the BCPs (Cremer & Kraka, 1984). The kinetic energy density $G(\mathbf{r})$ is related to the potential energy density $V(\mathbf{r})$ through the local virial theorem (Bader, 1994). In covalent bonds $V(\mathbf{r})$ is strongly negative and dominates the total energy density, defined by $H(\mathbf{r}) = G(\mathbf{r}) + V(\mathbf{r})$. In closed-shell interactions $G(\mathbf{r})$ dominates and $H(\mathbf{r})$ becomes positive. The ratio $G(\mathbf{r})/\rho(\mathbf{r})$, the kinetic energy density per electron, is generally larger than 1 for closed-shell interactions and smaller than 1 for shared interactions. Similarly a more negative ratio $H(\mathbf{r})/\rho(\mathbf{r})$ indicates a greater shared character of the interaction (Gatti, 2005; Macchi & Sironi, 2003).

The relevant values for the Zn—S bonds are listed in Table 5. The experimental values are obtained with the Kirzhnitz approximation (Kirzhnitz, 1957; Abramov, 1997) for $G(\mathbf{r})$

Table 5
Topological properties at the BCPs in the bonds involving Zn.

First line experiment, second line theory.

Bond	Length (Å)	Rho (e Å^{-3})	Laplacian (e Å^{5})	G (a.u.)	V (a.u.)	H (a.u.)	G/ρ (a.u.)	H/ρ (a.u.)
Zn—S1	2.259 (1)	0.40 (1)	5.1 (1)	0.06	−0.07	−0.01	1.03	−0.14
		0.54	3.6	0.07	−0.10	−0.03	0.84	−0.38
Zn—S2	2.275 (1)	0.47 (1)	3.6 (1)	0.06	−0.08	−0.02	0.84	−0.30
		0.52	3.5	0.06	−0.09	−0.03	0.83	−0.36
Zn—N1	2.105 (1)	0.55 (1)	6.1 (1)	0.09	−0.11	−0.02	1.06	−0.27
		0.47	6.4	0.08	−0.09	−0.01	1.12	−0.17
Zn—N2	2.118 (1)	0.34 (1)	8.1 (1)	0.08	−0.07	0.01	1.50	−0.08
		0.45	6.1	0.07	−0.08	−0.01	1.10	0.16

Table 6
Charges on ligands (e).

First line experiment, second line theory.

	XD	Hirshfeld charges	Bader
Thiolate ligand 1	−0.39	−0.21	−0.34
		−0.45	−0.57
Thiolate ligand 2	−0.19	−0.08	−0.26
		−0.45	−0.57
Phenanthroline	−0.30	−0.11	−0.51
		+0.48	+0.18

combined with the local virial theorem. The total energy density for the Zn—S bonds is slightly negative. In the case of Zn—N2 it becomes slightly positive, indicating a shared interaction. The theoretical ratio $G(\mathbf{r})/\rho(\mathbf{r})$ is less than unity for the Zn—S bonds (0.84, 0.84), but higher than 1 (1.12 and 1.10) for both Zn—N bonds. Experimental values of $H(\mathbf{r})/\rho(\mathbf{r})$ are negative for Zn—S (−0.14/−0.30 a.u.) and for Zn—N1 (−0.273 a.u.), while for Zn—N2 it is slightly positive (0.160 a.u.). The value for Zn—S2 (−0.30 a.u.) is more negative than that for Zn—S1 (−0.14 a.u.), in agreement with the less positive value for the Laplacian at the BCP, opposite what would be expected from the bond length alone. It should be noted that the theoretical values refer to the experimental geometry in the crystal. When the geometry of the isolated molecule is subsequently optimized, the Laplacian values at the Zn—S BCPs are in agreement with the bond lengths.

5. Net charges and relation to photocrystallography

Experimental atomic charges are summarized in Table S3 of the supporting material. They have been evaluated by topological integration over the atomic basins as defined in the AIM theory (Bader, 1994) and according to the stockholder concept of Hirshfeld (Hirshfeld, 1977). Hirshfeld charges on the Zn atom from both refinements 2 and 3 are in reasonable agreement with those from theory (Table 4), and positive as expected for Zn. As is common, the topological analysis leads to much larger magnitudes of the charges than the Hirshfeld analysis. According to both partitioning methods the phenanthroline ligand carries a negative charge (−0.11 e/−0.51 e) according to experiment, while the theory predicts a positive charge (0.43 e/0.18 e). The toluenethiol ligands are negatively charged (Table 6) according to both experiment and theory. While according to theory the two thiolate ligands have the same negative charge in the isolated molecule, there is a difference between the two according to experiment, the ligand involved in the π–π interaction (thiolate ligand 2) having a smaller charge than the free ligand. Time-dependent density-functional (TDDFT) calculations and photocrystallographic experiments to be reported elsewhere (Schmoekel *et al.*, 2010) indicate the long-wavelength emission of this class of compounds to be due to a thiolate to phenanthroline LLCT. The net charges observed in this study are in agreement with this conclusion.

6. Conclusions

The initial refinement of the asphericity of the Zn charge density with electron-density multipoles only leads to a misleading result which lacks physical significance. Much of the asphericity is due to anharmonic motion, significant even at liquid nitrogen temperatures. A joint refinement of anharmonic and charge-density parameters is possible and leads to correlations which are significantly smaller than those of an exploratory study reported 20 years ago, a difference attributed to the dramatic improvement in data quality. The two thiolate ligands are not equivalent, one being π-stacked with the phenanthroline ligand, as evidenced by the geometry and a bond-path connecting the two ligands in the charge density. This non-equivalence leads to different charges on the two ligands, the π-stacked thiolate being closer to neutral. The results do not provide a preference for either of the thiole ligands being the source of the transferred electron density. This result is in agreement with theoretical calculations, which show comparable oscillator strengths for charge transfer from the two ligands. The work illustrates the application of X-ray charge-density analysis as a complementary technique in the elucidation of photochemical properties in crystals.

The authors would like to thank Dr Louis Farrugia and Piero Macchi for helpful suggestions concerning the proper refinement of the Zn asphericity. Support of this work by the National Science Foundation (CHE0843922) is gratefully acknowledged.

References

Abramov, Yu. A. (1997). *Acta Cryst.* A**53**, 264–272.
Bader, R. (1994). *Atoms in Molecules. A Quantum Theory*. New York: Oxford University Press.
Blessing, R. H. (1997). *J. Appl. Cryst.* **30**, 421–426.
Bruker (1999*a*). *SMART*, Version 6.01. Bruker AXS Inc., Madison, Wisconsin, USA.
Bruker (1999*b*). *SAINT-Plus*, Version 6.01. Bruker AXS Inc., Madison, Wisconsin, USA.
Cheeseman, J., Keith, T. A. & Bader, R. F. W. (1992). *AIMPAC*. Technical Report. McMaster University, Hamilton, Ontario, Canada.

Cremer, D. & Kraka, E. (1984). *Angew. Chem. Int. Ed.* **23**, 627–628.
Cremers, T. L., Bloomquist, D. R., Willett, R. D. & Crosby, G. A. (1980). *Acta Cryst.* B**36**, 3097–3099.
Crosby, G. A., Highland, R. G. & Truesdell, K. A. (1985). *Coord. Chem. Rev.* **64**, 41–52.
Frisch, M. J. *et al.* (2009). *GAUSSIAN*09, Revision A.2. Gaussian, Inc., Wallingford CT, USA.
Gatti, C. (2005). *Z. Kristallogr.* **220**, 399–457.
Hansen, N. K. & Coppens, P. (1978). *Acta Cryst.* A**34**, 909–921.
Highland, R. C., Brummer, J. G. & Crosby, C. A. (1986). *J. Phys. Chem.* **90**, 1593–1598.
Hirshfeld, F. L. (1976). *Acta Cryst.* A**32**, 239–244.
Hirshfeld, F. L. (1977). *Theor. Chim. Acta*, **44**, 129–138.
Jordan, K. J., Wacholtz, W. F. & Crosby, G. A. (2002). *Inorg. Chem.* **30**, 4588–4593.
Kirzhnitz, D. A. (1957). *Sov. Phys.* **5**, 64–72.
Macchi, P. & Sironi, A. (2003). *Coord. Chem. Rev.* **238–239**, 383–412.
Mallinson, P. R., Koritsanszky, T., Elkaim, E., Li, N. & Coppens, P. (1988). *Acta Cryst.* A**44**, 336–343.
Ngan, T.-W., Ko, C.-C., Zhu, N. & Yam, V. W.-W. (2007). *Inorg. Chem.* **46**, 1144–1152.
Novakovic, S. B., Bogdanovic, G. A., Fraisse, B., Ghermani, N. E., Bouhmaida, N. & Spasojevic de Bire, A. (2007). *J. Phys. Chem. A*, **111**, 13492–13505.
Schmoekel, M. S., Benedict, J. B., Kaminski, R. & Coppens, P. (2010). In preparation.
Sheldrick, G. M. (2008). *Acta Cryst.* A**64**, 112–122.
Spasojevic de Bire, A., Bouhmaida, N., Kremenovic, A., Morgant, G. & Ghermani, N. E. (2002). *J. Phys. Chem. A*, **106**, 12170–12177.
Volkov, A., Macchi, P., Farrugia, L. J., Gatti, C., Mallinson, P. R., Richter, T. & Koritsánszky, T. S. (2006). *XD*2006, Rev. 5.34. University at Buffalo, State University of New York, NY, USA.
Volkov, A. V. (2005). *WFN*2*PLOTS*. University at Buffalo, State University of New York, NY, USA.